Bulgarian Chemical Communications, Volume 48, Special Issue E (pp. 365 - 372) 2016

Nanostructured carbon materials as promoters of energy storage

P. Lesnicenoks[1,2], M. Zvine[3], A. Januskevica[3], V.L. Muzikants[3], M.K. Jurjans[3], K. Kaprans[1], A. Volperts[4], G. Kucinskis[1], G. Bajars[1], G. Dobele[4], J. Kleperis[1*]

[1]*Institute of Solid State Physics, University of Latvia, 8 Kengaraga str, Riga, LV-1063, Latvia;*
[2]*Faculty of Materials Science and Applied Chemistry, Riga TU; 14/24 Azenes str, Riga, LV-1048, Latvia;*
[3]*Riga French Lyceum, 8 Meness str, Riga, LV-1013, Latvia;*
[4]*Latvian State Institute of Wood Chemistry; 27 Dzerbenes str, Riga, LV-1006, Latvia*

Nanostructured carbon materials in recent years have proved to be promoters of energy storage in different technologies – electricity storage in lithium ion batteries and supercapacitors, and hydrogen storage in solid state materials. Our research results on nanostructured carbon materials in lithium ion batteries, electrodes for supercapacitors and hydrogen storage vessels, confirms the indispensable role of it. The commercial and self-made nanostructured carbon materials (black carbon, graphite flakes, graphene oxide, wood-based activated carbons, few layer graphene stacks) are used as additives and selected results reported. $LiFePO_4/C$ composite material as cathode for lithium ion battery is prepared and electrochemical tests are performed to determine the charge capacity and analyse the role of additives. Research on activated wood-based carbon for electrodes of supercapacitors with organic electrolyte showed that specific capacity and ohmic losses of electrode is influenced by the properties of the pores in carbon structures. The ratio of raw material to activator and appropriate activation temperature are most important factors to obtain optimal pore dimensions. Few layer graphene stacks (FLGS) without and with different interlayer ion additives are synthesized and tested for electrodes in supercapacitors as well as solid state sorption media for hydrogen storage. It is found that non-reduced FLG is able to realize sorption on defects mostly at cryogenic temperatures, and this is also true for non-intercalated graphene at low hydrogen pressures. Nevertheless, Li intercalation allows to reach higher values of bind hydrogen (around 1 wt%) at higher temperatures.

Key words: carbon, nanoporous, few layer graphene stacks, energy storage, hydrogen storage

INTRODUCTION

In order to reduce global climate change by limiting CO_2 emissions, it is necessary to switch from continuous power (electricity) production by burning fossil fuels (coal, oil, gas) to the unsteady energy generation from local renewable energy sources (sun, wind, water in rivers). Therefore nowadays reliable energy storage systems are critically needed to store and supply power in continuous manner. Electricity and hydrogen are two comparable energy carriers, and in order to be able to meet humanity's demand for energy, electricity storage and hydrogen storage methods are researched.

Already for years electricity is stored in large quantities pumping water in basins of hydro-electric power stations, in flywheels, in vessels with compressed air etc. [1]. Low scale electrochemical energy storage systems are electrochemical capacitors (also supercapacitors), rechargeable batteries, and fuel cells [2]. Pristine and intercalated carbon nanostructures have attracted significant research interest for electrochemical energy storage systems – supercapacitors – as electrode materials due to their developed structures with large specific surface area, excellent electrical conductivity and electro-catalytic activity [2, 3]. Carbon nanostructured materials such as fullerenes, nanotubes, nanowires, graphene are most researched materials in this field in the last decades [4, 5]. Smaller attention is given to organic nanoporous charcoals [5].

After the commercialization of the Li-ion battery with metallic lithium anode and numerous self-ignition cases in hands of consumers, carbon-based anode for rechargeable batteries have gained extensive attention [6]. Here carbon porous/layered structures are reversibly absorbing/desorbing lithium ions at low electrochemical potentials. Graphite can intercalate one Li atom per carbon ring: $Li^+ + e^- + C_6 \leftrightarrow LiC_6$ corresponding to 372 mAh/g theoretically (comparing to about 3800 mAh/g for Li metal). With some amorphous carbons Li can intercalate at even higher capacity, corresponding to an obtainable stoichiometry of LiC_3. Therefore, by replacing Li metal anodes with carbon nanomaterials in Li batteries, there is 90% decrease of anode capacity, but the advantages are increased stability and prolonged cycle life [2]. The most important cathode materials for commercially available Li-ion batteries are layered oxides having potential 3.5–4 V (versus Li electrode) $LiCoO_2$, as well as $LiMn_2O_4$ [7], $LiFePO_4$ [8] and $LiMn_xLi_yCo_zO_2$ [9] with capacities of 150, 120, 155

---

[*] To whom all correspondence should be sent:
janis.kleperis@h2lv.eu

and 160 mAh/g, respectively. As a rule, the electrodes from oxide nanocrystals are formed by mixing them with various carbon nanostructured materials to improve the electrical and heat conductivities and mechanical strength [10].

Activated carbons are produced from wood charcoal with developed porous structure and previously used as sorbents in many areas, but nowadays also in membrane technologies for separation of rare earth metals, in metallurgy, in electronics, in electrochemistry, aerospace, nuclear energy. Pyrolysis and activation are two basic technologies to obtain activated carbons from extremely wide range of precursors: wood chips, cellulose and lignin, lignocelluloses, nut shells, straw, peat, husks, etc. The chemical activation is a widely used method to produce activated carbons with developed porosity for electrodes in electric double layer capacitors or supercapacitors [11]. The chemical activation allows possibility to synthesize carbonaceous materials with very high specific surface, close to the theoretical limits for carbon materials.

Hydrogen is important energy carrier for mobile as well as stationary applications and storage is important consideration in all applications of hydrogen energy technologies. High pressure (up to 70 MPa) vessels are used to store 5-6 kg of hydrogen in passenger car – enough for 500-600 km travel [12]. Liquid hydrogen has a very low temperature (20 K) and mostly is stored for space applications. Hydrogen can also be stored in solid materials: metal hydrides, chemical hydrides, porous materials are the most known ones [12]. Only high density alloys forms hydrides at room temperature ($LaNi_5$, Ti_2Fe), but lighter metals Mg, Li form hydrides at high temperatures and/or high pressure [12]. In metal hydrides hydrogen atom is incorporated in crystal lattice structure, but in microporous materials molecular hydrogen is absorbed in pores leading to an increase in the density of hydrogen compared to the hydrogen compressed in the gas phase [12]. Adsorption on surfaces and in pores occurs primarily at relatively low temperatures (≈100 K) and in micropores (below 2 nm). The porous materials being considered for physisorbed molecular hydrogen storage are predominantly microporous [12,13] with pore dimensions less than 0.7 nm (close to the size of a single hydrogen molecule).

Carbonaceous materials are attractive candidates for hydrogen storage because of a combination of adsorption ability, high specific surface area, layered or pore microstructures, and low mass density. In spite of extensive results available on hydrogen uptake by carbonaceous materials, the actual mechanism of storage still remains a mystery [13]. Hydrogen molecule can interact with carbon surface through van der Waals attractive forces (physisorption), or dissociate in atoms and are chemisorbed. The physisorption of hydrogen limits the hydrogen-to-carbon ratio to less than one hydrogen atom per two carbon atoms (i.e., 4.2 wt. %), while in chemisorption, the ratio of two hydrogen atoms per one carbon atom (8.4 wt. %) is reported in the case of polyethylene [13–15]. Physisorbed hydrogen normally has a binding energy on the order of 0.1 eV, while chemisorbed hydrogen has C–H covalent bonding, with a binding energy of more than 2-3 eV [13]. The graphene has some advantages for hydrogen storage because the sp^2 covalent-bonding arrangement of the carbon atoms in the honeycomb structure allows efficient binding to hydrogen atoms [16]. Graphene is stable, light, with high theoretical surface; it is mechanically flexible, and it is possible to charge/discharge it at room conditions through hydrogen-carbon binding on local curvatures [16].

In this article our research results on the role and properties of nanostructured carbon materials in lithium ion batteries, electrodes for supercapacitors and hydrogen storage materials have been summarized.

EXPERIMENTAL SYNTHESIS OF MATERIALS AND SAMPLES

Two types of nanostructured carbons are synthesized – activated carbon (AC) from Latvian alder wood [17] and few layer graphene stacks (FLGS) [18]. AC synthesis consists of two stages of thermal treatment [17] – carbonization of raw material in Ar atmosphere (400 °C, 150 min) at the first stage, and carbonization with activator (NaOH in Ar flow (600-800 °C, 120 min) at the second stage. The pyrolysis product was washed with deionized water, demineralized with hydrochloric acid, washed with deionized water until neutral pH and dried overnight at 105 °C. In order to obtain few layer graphene (FLG), the electrochemical exfoliation was performed, using graphite industrial waste rod as working electrode 18]. Different pulse sequences, amplitudes and filling factors were used to find optimal parameters of exfoliation process. Important step is purification of processed raw material – single sheets are lightest and can be easy separated with centrifuge or sedimentation. To guaranty higher degree of reduction of FLGS, filtered material was annealed in Ar/H_2 (95:5) gas flow at 300°C for 3 hours.

Carbon in battery electrodes

To design cathode from $LiFePO_4$, different carbon additives are used. $LiFePO_4$ was obtained in a two-step solution reaction of lithium dihydrogen phosphate LiH_2PO_4 and iron oxalate $FeC_2O_4{\cdot}2H_2O$ (all from Sigma-Aldrich, ≥99.9%) in de-ionized water. Graphene oxide was added to the synthesis at various steps and then thermally reduced in order to study the influence that the grain structure of $LiFePO_4$/reduced graphene oxide (rGO) has on the electrochemical properties of the composite.

Thick films of $LiFePO_4/C$ cathode are made from $LiFePO_4$, conducting additive (carbon black or acetylene black, graphite flakes, Latvian wood charcoal, few layer graphene stacks) and binder (polyvinylidene difluoride PVDF and n-methyl-2-pyrrolidone NMP 50%:50%) in proportions 75:15:10 and grounded 30 min in ball mill (RETSCH Mixer Mill MM 200) then casted on aluminium foil and dried 24 h at 60 °C in air and 3h at 100 °C in an argon atmosphere.

Water suspension of graphene oxide was used for electrophoretic deposition (EDP) of thick graphene films for anode in lithium ion battery [19]. Before the EPD process the graphene oxide suspension was sonicated for 1 h in order to ensure homogenous dispersion. Electrodes used for EPD process were 316 stainless steel plates and the distance between the two electrodes was 10 mm; electric field 30 $V{\cdot}cm^{-1}$ was applied using DC power supply Agilent Technologies N5772A). Thermal reduction of as-deposited graphene oxide (GO) films was performed by heating at 700 ºC in argon atmosphere. The measurements of synthesized electrodes (area 0.8 cm^2) were performed in Swagelok type two electrode cells with metallic lithium as a reference and a counter electrode, and $LiPF_6$ in ethylene carbonate and dimethyl carbonate mixture (volume ratio 1:1) as an electrolyte. The cell was assembled in an argon filled glove box.

Carbon in supercapacitors

Two methods were used to prepare electrodes from nanostructured carbons for supercapacitor research [17, 20]. ***In one of them*** the AC was first mixed with ethanol, then a binder – a water suspension of PTFE F-4D powder (10 % from mass of dry electrode) was added. The resulting mixture was treated in rollers, electrode was prepared on thermally expanded graphite sheet (200 μm), than it was dried and impregnated with 4.9 M H_2SO_4 water solution. Cellulosic separator NKK TF 4030 (10 μm) was used to make a supercapacitor with electrode area 4.15 cm^2. The assembled supercapacitor was pressed under 10 atm pressure in a dry box. ***Second method*** uses aluminium foil plate as current collector and substrate, which is first treated with $CuSO_45H_2O$ and NaCl etching solution in order to remove oxides [20]. Different FLGS powders (pristine and intercalated with Na and Li) as well as AC powder were mixed with poly-vinyl acetate (PVAc) and the obtained paste gently was applied to etched aluminium electrode using small tungsten blade and left to dry for 1-2 days. Capacitor was made from two equal electrodes, one from three tested separators (Celgard-2400 membrane, Rossmann rayon/cellulose fabric and Whatman glass fibre filter) and one from following electrolytes – 1 M water solutions of NH_4Cl, NaCl, $LiPF_6$, KOH, and Na_2SO_4. Cut electrodes with an area of 1 cm^2 and separator soaked with electrolyte were put in plastic pocket and laminated directly with a laminator or on a hotplate.

Carbon for hydrogen storage

Two different nanostructured carbon materials were tested – activated carbon AC from Latvian alder wood [17] and few layer graphene stacks FLGS – pristine and intercalated with Na, Mg and Li [18].

METHODS USED IN RESEARCH

The crystal structure was examined by x-ray diffraction (XRD) using a Philips X'Pert Pro MPD diffractometer with CuKα radiation. Molecular structure was investigated by Raman spectroscopy, using an Advantage-785 spectrometer with a laser wavelength of λ=785nm and InVia Renishaw micro-Raman spectrometer equipped with argon laser (514.5 nm, 10 mW). Surface morphology of synthesized samples was characterized by scanning electron microscopes (SEM) - Carl Zeiss EVO 50 XVP, Hitachi S-400N, Tescan Lyra and table-top SEM Phenom Pro.

Pore structure was assessed by N_2 adsorption at 77 K (Kelvin 1042, Costech Instruments). Pore volume was calculated by using Dubinin-Radushkevich and Brunauer– Emmet–Teller (BET) theories and N_2 sorption isotherms [17]. Carbon content in $LiFePO_4/C$ samples was determined via thermogravimetric analysis (TGA).

Electrochemical measurements were carried out with potentiostat Voltalab PGZ-301 (and partly with potentiostat ELLINS 30-S) using open circuit potential scanning, electrochemical impedance, cyclic voltammetry and chronopotentiometry methods. Charge-discharge measurements of electrodes for batteries and supercapacitors were done with various current densities in a range of 1-100 $\mu A/cm^2$. Capacities shown were calculated ether using the dry mass of an electrode without the electrolyte or normalized per 1 cm^2 area.

Hydrogen adsorption measurements were performed with Sievert's type device, attached to Mass spectrometer RGA-100, in which cryogenic cooling as well external heating is possible in temperature range +/- 200^o C. Two gases, hydrogen and helium, are applied to the sample, firstly with He calibrating sample volume, then measuring H_2 adsorption-desorption values in powdered samples. The volume of camera is 94 cm^3, both gases are filled with pressure 3.2 ±0.1 bar at room temperature (20^o C). Pressure sensor is situated outside from camera to be heated/cooled therefore pressure values measured at higher and lower temperatures are relative. When absolute values of hydrogen adsorbed in sample are calculated, temperature correction in differential pressure values are taken into account.

RESULTS AND DISCUSSION

Carbon in battery electrodes

XRD analysis displays all peaks characteristic to the orthorhombic $LiFePO_4$ crystal lattice and Pnma space group, no impurities have been observed [21, 22]. Raman spectroscopy shows carbon D and G bands located at 1350 cm^{-1} and 1600 cm^{-1} respectively. No significant differences in Raman spectra can be observed between samples with and without reduced graphene oxide (rGO), therefore it can be concluded that rGO sheets coated on $LiFePO_4$ are very thin. TGA shows that $LiFePO_4/C$ consists of 1.1 % carbon and confirms that $LiFePO_4/C/rGO$ additionally contains almost 3 % rGO. SEM image of $LiFePO_4/C/rGO$ is shown in Fig.1.

The observation of single and few layer graphene in SEM is complicated, and often advanced SEM equipment is necessary, as one or few layer graphene can be nearly transparent for high energy electron beams [21]. Nevertheless, rGO sheets have been observed in all prepared $LiFePO_4/C$ samples. The grain sizes are approximately 100 – 700 nm, the obtained powders are noticeably porous - the average pore volume is 56 mm^3/g. The BET surface area is not sensitive to additive rGO, therefore it is similar to all prepared $LiFePO_4/C$ samples – ~30 m^2/g. The presence of rGO in $LiFePO_4/C/rGO$ composite has caused an increase of the already high rate capability of $LiFePO_4/C$ – up to 163.5 mAh/g at 0.1 C (here 1 C = 170 mA/g). The rGO-wrapped $LiFePO_4/C$ grains in sample $LiFePO_4/C/rGO$ have also provided significant rate capability improvements (Fig.2).

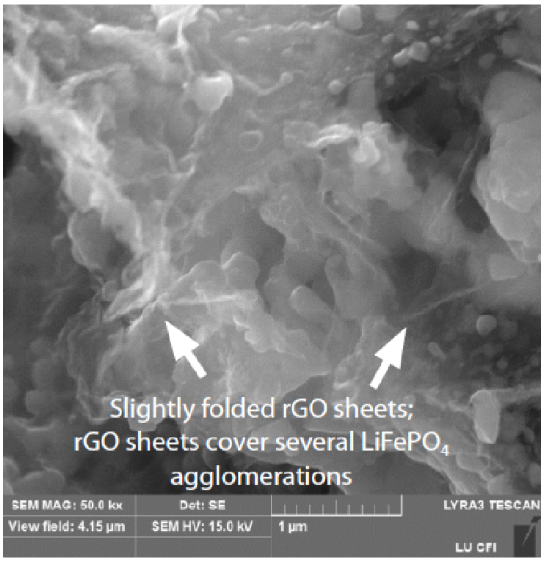

Fig.1. SEM image of $LiFePO_4/C/rGO$ [22].

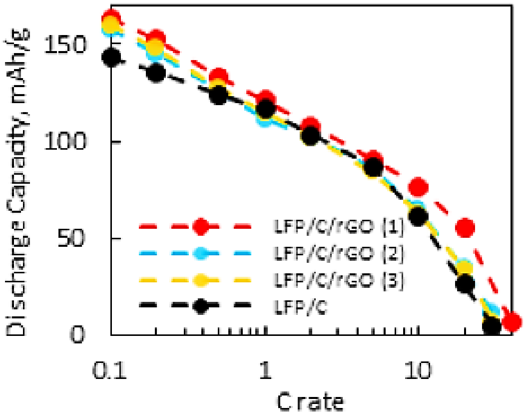

Fig.2. The rate capabilities of the obtained composites [22].

The increase of the galvanostatically measured charge capacities above 5 C rate for rGO containing cathodes is seen due to the electron – conducting network created by rGO in $LiFePO_4/C$ improving the electron transport in the cathode. It seems that the rate capability is improved more if the graphene oxide (GO, rGO precursor) is added to the synthesis at the earliest possible stage (sample LFP/C/rGO (1)). It is also worth noting that the capacity is increased not only at the higher charge and discharge rates, but also lower rates. The increase of the amount of the stored lithium in $LiFePO_4$/C/rGO and other obtained $LiFePO_4$ – rGO composites is most likely also due to the increased fraction of the electrochemically active $LiFePO_4$ particles as a result of the rGO electron-conducting network. It is worth noting that recently an additional Li storage capacity due to the newly formed $LiFePO_4$ – rGO composite has been observed by Hu et al. [23], and such contributions also cannot be ruled out in this work.

Other nanostructured carbon additives (commercial carbon black and AC [17]) were tested [24]. From the charge – discharge graphs it can be concluded that the model battery in which carbon black has been used as an electron conducting additive for the $LiFePO_4$ electrode displays a higher charge capacity - 109.5 mAh/g) as compared with model battery where AC is used as additive to $LiFePO_4$ – 97 mAh/g [24]. This result can be explained with differences in microstructures of both carbon forms - carbon black is like a sponge capable of covering the $LiFePO_4$ grains and providing better electrical conductivity between them, whereas AC mostly consists of large grains with rather sharp edges (Fig.3).

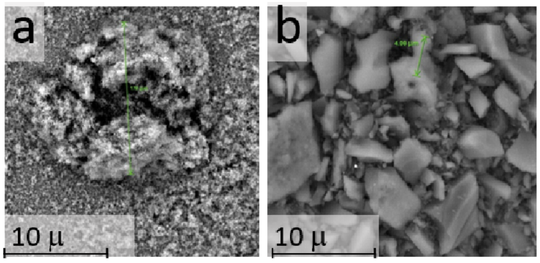

Fig.3. SEM image of carbon black (a) and activated carbon (b) materials [24].

Electrophoretically coated GO films can be used as anodes in lithium ion batteries. XRD analysis of electrophoretically prepared rGO film (Fig.4) exhibits a characteristic peak of graphene at 26.5° (002), which was not observed for GO [19]. The characteristic peak of GO powder at 11° was not observed for electrophoretically coated and reduced film on steel substrate (upper curve, Fig.4). It means that most of the GO was successfully converted to graphene by thermal reduction of the electrophoretically deposited GO films. The gravimetric charge capacity at slow discharge rate (I = 0.8 mA) reaches high value ~ 1120 mAh/g, but increasing of discharge rate causes the gradual decrease of capacity.

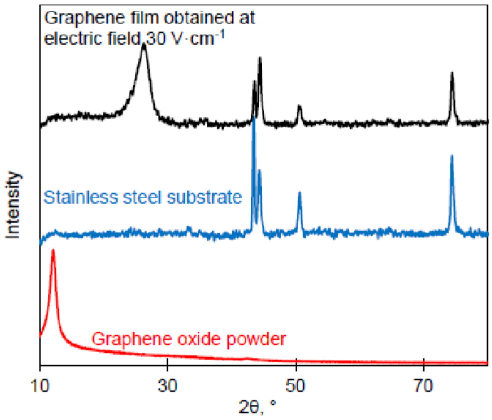

Fig.4. XRD patterns for GO, steel substrate and rGO or graphene film [19].

At much higher discharge rate (I = 2 mA) capacity falls to ~ 620 mAh/g and after 50 cycles stabilizes at ~ 530 mAh/g [19]. The Coulombic efficiency for first 50 cycles of rGO electrode exceeded over 85 % and further decrease of capacity during the cycling is negligible. Much lower capacities are measured for anode made from commercial graphite flakes - 135.6 mAh/g, and even less is determined for anode made from FLGS - 111.5 mAh/g [24]. The results show that electrophoretic deposition compares favourably with the classical thick film technology in the case of lithium ion battery anode preparation.

Carbon in supercapacitors

Results of capacitor electrodes made from AC according to methodology developed by Volperts et al. [17, 25] showed that highest values of specific capacitance is achieved for materials obtained at low carbonization temperatures – 600 °C and 700 °C – the capacitance is 330 F/g and 320 F/g correspondingly. With increase of activation temperature, specific capacity decreases, although total volume of pores increases. This capacity decrease with increase of activation temperature corresponds to decrease of micropore volume (0.8 nm – 1.5 nm) proportion in porous structure of activated carbons. Few layer graphene stacks (FLGS) is a different nanostructured carbon material made according to the methodology developed by Lesnicenoks et al. [18]. The presence of graphene is confirmed by Raman spectroscopy

(Fig.5). This spectroscopy is the most commonly used method in the characterization of the quality of graphene, as well as separation of graphite from graphene. A single Raman peak at 1580 cm^{-1}, called the G peak is characteristic to natural single-crystal graphite. It is formed by in-plane C−C bond stretching (E_{2g}) mode of sp^2 hybridized carbon atoms.

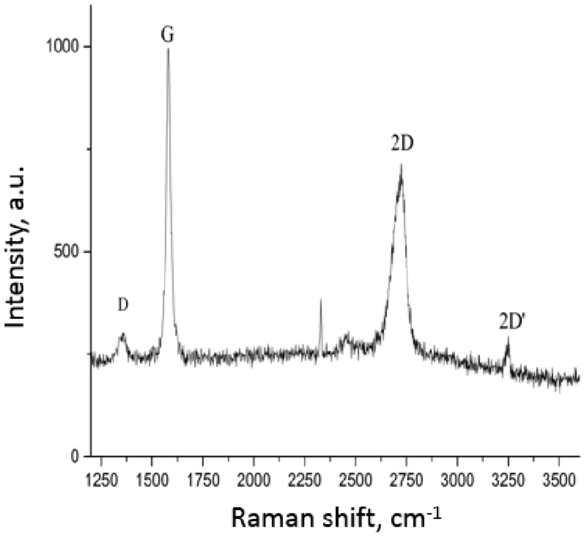

Fig.5. Raman spectra of FLGS powder material.

In a perfect graphite crystal the first-order vibrational mode of the D band is forbidden because of selection rules, but if the long range order of the crystalline material is lost and the graphite becomes polycrystalline (splits in sheets), D peak appears at 1358 cm^{-1}. The relation between width and intensities of G and 2D peaks is characterized with the number of graphene layers and sample quality. High number of layers in stacks is responsible for the width of 2D peak at 2685 cm^{-1}.

Cyclic voltammetry results (Fig.6) confirms that from the tested separators – "Celgard 2400" membrane, "Rossmann" rayon/cellulose fabric and "Whatman" glass fibre filter - the last two show higher current values 1 M solution of NH_4Cl is used as electrolyte [20] in all cases). The dependence from membrane material could indicate insufficient ionic transport through the separator. The role of separator in a perfect case is to only separate both electrodes [26]. However, in real life different separators might lead to different amounts of electrolyte being used, therefore not allowing a proper wetting of the electrodes. It should also be noted that all three of the membranes have different thicknesses; in addition, samples were encapsulated using a commercial laminating device (temperature +110 °C) and plastic covers, which can influence materials more sensitive to temperature, as the Celgard 2400 membrane is made of polypropylene.

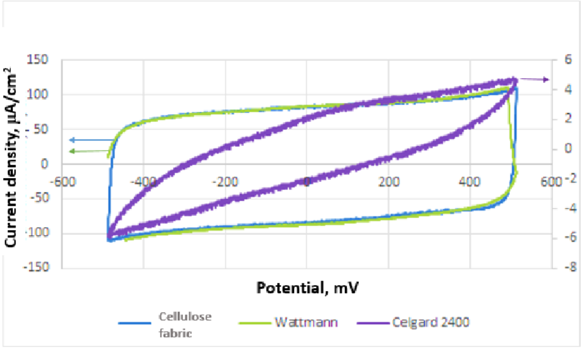

Fig.6. Volt-amperic characteristics (scan rate of potential – 50 mV/s) of capacitors with FLGS electrodes and different separators.

FLGS were tested as electrodes in capacitors with difference in formation of active material as described above (using PVAc as binder instead of PTFE), and several measurements were made.

From charge-discharge curves the capacity values are calculated for all measured samples (Table 1).

Table 1. The values of measured capacities.

Electrode material	Electrolyte	Capacity ± 0.01 mF/cm^2
AC	KOH	0.37
AC	NH_4Cl	0.86
FLG,	NaCl	0.26
FLG isolated	NaCl	0.95
Na FLG	$NaSO_4$	4.47
Li FLG	$LiPF_6$	$2.28 \cdot 10^3$

From capacitor volt-amperic (Fi.6) and charge-discharge curves (not shown here) it can be seen that they are partly reminiscent to batteries and partly to capacitors. Since the graphene electrodes can be used in lithium-ion batteries as the anode and cathode, apparently we have obtained a hybrid battery-supercapacitor, especially in case using $LiPF_6$ electrolyte; this sample also has the largest capacity (Table 1). The hybrid battery is combination of different types of energy storage in one source [27].

The reason of such remarkable difference between capacitors with inorganic and organic electrolytes may be caused by the applied binder (PVAc).

Carbon for hydrogen storage

Comparing the hydrogen adsorption performance of activated carbon (AC) from Latvian alder wood with few layer graphene stacks FLGS intercalated with Li (Fig.7) it can be seen that activated carbon (brown line) starts to adsorb hydrogen at temperature of approx. 230 K.

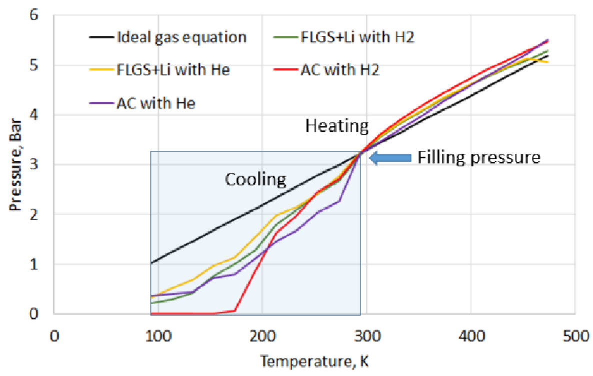

Fig.7. Pressure – Temperature characteristics of two samples (AC and FLGS+Li) in two different atmospheres – helium and hydrogen.

Calculated value of absorbed hydrogen mass in AC sample approaches 1.3 wt% and is promising value for further research and potential applications. Detailed analysis of the pressure and temperature output data for this sample (Fig.8) shows pronounced hydrogen absorption region (coloured circle) with temperature and pressure oscillations, which indicate an exothermic reaction (heat is released).

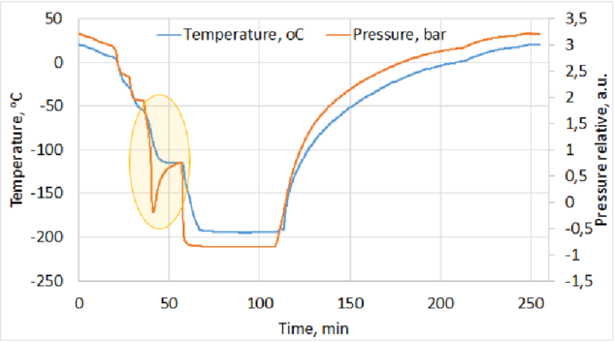

Fig.8. Pressure and Temperature as function of time during cooling and heating sample AC in hydrogen atmosphere.

If we consider mechanisms such as metal hydride formation, Li should not be favourable as low temperature hydride, but in our system – intercalated graphene surfaces, we are more concerned with stabilisation of defects in FLGS plates, thus Li FLGS is still considered because preliminary results (Fig.7) show small but positive value – 0.1 wt% of adsorbed hydrogen starting from 170 K.

CONCLUSIONS

Carbon in battery electrodes

From the charge – discharge graphs it can be concluded that the cathode material $LiFePO_4$/carbon black has a higher charge capacity as cathode material with active carbon additive (109.5 and 97 mAh/g accordingly). The presence of rGO in $LiFePO_4$/C/rGO composite has caused an increase of the already high rate capability of $LiFePO_4$/C – up to 163.5 mAh/g at 0.1 C (here 1 C = 170 mA/g). The rGO-wrapped $LiFePO_4$/C grains in sample $LiFePO_4$/C/rGO have also provided significant rate capability improvements. Electrophoretically deposited GO films can be used as anodes in lithium ion batteries. The gravimetric charge capacity at slow discharge rate (I = 0.8 mA) reaches high value ~ 1120 mAh/g, but at higher discharge rate (I = 2 mA) capacity falls to ~ 620 mAh/g and after 50 cycles stabilizes at ~ 530 mAh/g. Much lower capacities are measured for anode made for commercial graphite flakes - 135.6 mAh/g, and even less is determined for anode made from FLGS - 111.5 mAh/g.

Carbon in supercapacitors

Results of capacitor electrodes made from activated carbon showed that highest values of specific capacitance 330 F/g and 320 F/g are achieved for materials obtained at low carbonization temperatures – 600 °C and 700 °C – correspondingly. From the tested separators - "Celgard 2400" membrane, "Rossmann" rayon/cellulose fabric and "Whatman" glass fibre filter - the last two show higher current values, when 1 M solution of NH_4Cl is used as electrolyte.

Carbon for hydrogen storage

Comparing hydrogen adsorption performance of activated carbon from Latvian alder wood with few layer graphene stacks FLGS intercalated with Li it can be seen that activated carbon starts to adsorb hydrogen at temperatures of approx. 230 K and reach value 1.3 wt%.

ACKNOWLEDGEMENT

All authors acknowledge financial support from Latvian Science Council (Collaboration Grant No 666/2014-2017).

REFERENCES

1 H. Ibrahim, A. Ilinca, J. Perron, *Renew. Sustain. Energy Rev.*, 12, 1221 (2008).

2 H.D. Yoo, E. Markevich, G. Salitra, D. Sharon, D. Aurbach, *Materials Today*, 17, No 3, 110 (2014).

3 Y. Wang, H. Wei, Y. Lu, S. Wei, E.K. Wujcik, Z. Guo, *Nanomaterials*, 5. No 2, 755 (2015).

4 M.D. Stoller, S. Park, Y. Zhu, J. An, R.S. Ruoff, *Nano Lett.* 8, 3498 (2008).

5 D. Saha, Y. Li, Z. Bi, J. Chen, J.K. Keum, D.K. Hensley, H.A. Grappe, H.M. MeyerI, S. Dai, M.P. Paranthaman, A. K. Naskar, *Langmuir*, 30, No 3, 900 (2014).

6 C. De las Casas, W. Li, *J. Power Sources*, 208, 74 (2012).

7 M.S. Whittingham, *Chem. Rev.*, 104, 4271 (2004).

8 J.B. Goodenough, *J. Power Sources*, 174, 996 (2007).

9 J.W. Fergus, *J. Power Sources*, 195, 939 (2010).

10 G. Kucinskis, G. Bajars, J. Kleperis, *J. Power Sources,* 240, 66 (2013.

11 M. Inagaki, H. Konno, O Tanaike, *J. Power Sources*, 195, 7880 (2010).

12 D. P. Broom, Hydrogen Storage Materials: Green Energy and Technology, Springer-Verlag London Limited, 2011.

13 M.U. Niemann, S.S. Srinivasan, A.R. Phani, A. Kumar, D.Y. Goswami, E.K. Stefanakos, *J. Nanomaterials*, 2008, 9 pages (2008).

14 B. Viswanathan, M. Sankaran, and M. A. Schibioh, *Bulletin of the Catalysis Society of India*, 2, 12 (2003).

15 M. G. Nijkamp, J. E. M. J. Raaymakers, A. J. van Dillen, and K. P. de Jong, *Applied Physics*, 72A, No 5, 619 (2001).

16 V. Tozzini and V. Pellegrini, *Phys. Chem. Chem. Phys.*, 15, 80 (2013).

17 A. Volperts, G. Dobele, J. Ozolins, N. Mironova-Ulmane, *Material Science and Applied Chemistry*, 31, 16 (2015).

18 P. Lesnicenoks, J. Zemitis, J. Kleperis, G. Chikvaidze, R. Ignatans, *Material Science and Applied Chemistry*, 31, 21 (2015).

19 K. Kaprans, G. Bajars, G. Kucinskis, A. Dorondo, J. Mateuss, J. Gabrusenoks, J. Kleperis, A. Lusis, *IOP Conf. Series: Materials Science and Engineering*, 77, 5 pages (2015).

20 M. Zvine, A. Januskevica, P. Lesnicenoks, G. Taurins, J. Kleperis. Abstracts of the 32nd Scientific Conference of Institute of Solid State Physics, University of Latvia, Febr 17–19, 2016, Riga, p. 65.

21 G. Kucinskis, G. Bajārs, J. Kleperis, J. Smits, *Environmental and Climate Technologies*, No 4, 53 (2010).

22 G.Kucinskis, The study of nanostructured bulk and thin film $LiFePO_4$ cathode materials for lithium-ion batteries. Summary of Doctoral Thesis, University of Latvia, 2015.

23 L.-H. Hu, F.-Y. Wu, C.-T. Lin, A. N. Khlobystov, L.-J. Li, *Nature Communications*, 4, 1687 (2013).

24 V.L. Muzikants, G. Kucinskis, M.K. Jurjans, G. Bajars, *Abstracts of the 32nd Scientific Conference of Institute of Solid State Physics*, University of Latvia, Febr 17–19, 2016, Riga, p. 66.

25 G. Dobele, D. Vervikishko, A. Volperts, N. Bogdanovich, E. Shkolnikov, *Holzforschung,* 67, No 5, 587 (2013).

26 A.C. Forse, C. Merlet, J.M. Griffin, C.P. Grey. J. Am. Chem. Soc. 2016, 138, 5731−5744.

27 A. Vlad, N. Singh, J. Rolland, S. Melinte, P.M. Ajayan & J.-F. Gohy. NATURE, SCIENTIFIC REPORTS, 2014, 4: 4315.